Satellite Determinations of the Relationship between Total Longwave Radiation Flux and Infrared Window Radiance

GEORGE OHRING AND ARNOLD GRUBER

National Environmental Satellite, Data and Information Service, NOAA, Washington, DC 20233

ROBERT ELLINGSON

Department of Meteorology, University of Maryland, College Park, MD 20742

(Manuscript received 2 July 1983, in final form 30 December 1983)

ABSTRACT

Nimbus-7 satellite observations are used to determine the relationship between the total longwave radiation flux and the radiance in the 10–12 μm infrared window. The total longwave fluxes are obtained from the earth radiation budget (ERB) narrow-field-of-view (NFOV) observations of total radiance; the IR window radiances are those measured by the Temperature Humidity Infrared Radiometer (THIR). Regression equations are obtained relating the total flux equivalent brightness temperatures to the radiance equivalent brightness temperature of the IR window. These empirical equations are compared to similar regression equations based on radiative transfer calculations for a large sample of atmospheric soundings. The latter theoretical equations are used by NOAA in the processing of IR window observations from operational polar orbiting satellites to obtain total longwave flux estimates. The observational results indicate that there is a very high correlation between the flux equivalent brightness temperature and the IR window radiance equivalent brightness temperature, and that the former can indeed be determined from measurements of the latter, thus validating the general NOAA approach. Tests on independent data suggest that rms flux errors of $\sim$11 W m^{-2} are to be expected for single applications of the empirical equations. The theoretical equations used by NOAA have an average positive bias of $\sim$13 W m^{-2} or a relative bias of $\sim$6% with respect to the ERB NFOV observations; the relative bias disappears at high flux values and increases with decreasing flux. A preliminary attempt to determine the cause of the discrepancy between the empirical and theoretical results indicates that a major factor may be the unrepresentativeness of the atmospheric soundings used in developing the theoretical regression coefficients.

1. Introduction

Although not designed for this purpose, the narrow spectral interval observations of the scanning radiometers (SR), and, more recently, the Advanced Very High Resolution Radiometer (AVHRR), on NOAA's polar orbiting satellites have been used to monitor the radiation budget of the earth–atmosphere system (ERB) (Gruber and Winston, 1978). The major purpose of these operational scanners is to provide visible (0.5–0.7 μm) and infrared (10.5–12.5 μm) cloud imagery for weather analysis and forecasting. Their use for radiation budget estimates is based on the high correlation between narrow- and broad-band radiation observations. The total longwave flux to space is obtained from the infrared window observations by applying a regression relationship based on computer simulations (Abel and Gruber, 1979); the planetary albedo is derived from the visible observation by assuming that the visible albedo is representative of the total albedo (Gruber, 1977; Gruber and Winston, 1978).

These radiation budget data have been used in a number of diagnostic studies (e.g., Ohring and Clapp, 1980; Hartmann and Short, 1980; Fromm *et al.*, 1982; Cahalan *et al.*, 1982; Winston and Krueger, 1977; Heddinghaus and Krueger, 1981; Liebman and Hartmann, 1982; Jensenius *et al.*, 1978). Comparison of large-scale averages of these ERB values with those based on broad-band observations indicates that while the albedos agree reasonably well, the longwave flux determinations appear to have a positive bias of $\sim$10 W m^{-2} (Ohring and Gruber, 1983).

It is important to determine the validity of these narrow-band estimates since they do provide a nearly continuous record since 1974. Furthermore, since the primary purpose of the narrow-band instrumentation is cloud imagery, such ERB estimates will be available far into the future. The same cannot be said about satellite instrumentation designed specifically for ERB observations. In the present study, the relationship between infrared window emission and total longwave flux is determined directly from simultaneous, colocated satellite observations of both. This empirical relationship is compared to the relationship based on simulations that is used operationally for processing the NOAA satellite narrow-band observations. Finally, possible causes of the differences between the empirical and operational relationships, and errors to be expected

from application of the empirical relationship to narrow-band observations, are discussed.

2. Data and methods

The data consist of total (4–50 μm) radiance observations by the narrow field of view (NFOV) scanning radiometer of the Earth Radiation Budget (ERB) experiment on Nimbus 7, and IR window (10–12 μm) observations by the Temperature Humidity Infrared Radiometer (THIR) on the same satellite. Detailed descriptions of Nimbus-7 instruments may be found in the *User's Guides* (NASA, 1978, 1982). The ERB radiance observations have a footprint at nadir of about 90 km; the THIR footprint is 7 km. Each of the ERB radiances is assigned to one of 18 630 approximately equal-area ($\sim$150 $\times$ 150 km) regions on the earth's surface, which are called sub-target areas (STAs). For another project, a cloud retrieval research program (Stowe *et al.*, 1978), the THIR observations had been averaged for each of these STAs. These average window radiances were used in the present study to compare with the ERB radiances. Only those ERB radiance observations whose fields of view fell completely within an STA and whose viewing angles were close to nadir (within 15°) were included in the present data set. These constraints were used in order to insure that the ERB radiance measurement and the THIR window radiance measurement were coincident in time and viewing angle, and were viewing approximately the same scene. Global data sets were prepared for three different days—26 November 1978, 17 April 1979, and 30 July 1979—each data set consisting of approximately 3000 matched ERB radiance and THIR window radiance observations.

In the operational processing of the NOAA satellite observations, estimates of total longwave radiation flux are obtained by application of a regression equation to the infrared window observations. This regression equation was derived from radiative transfer calculations of both total longwave flux and 10–12 μm window radiances for 99 atmospheric soundings covering a broad range of temperature and water vapor distributions, as well as overcast and clear conditions (Abel and Gruber, 1979). The derived regression equation is of the form

$$T_f = T_w(a + bT_w), \qquad (1)$$

where T_w is the radiance equivalent brightness temperature (K) in the IR window for a nadir view, and T_f is the flux equivalent brightness temperature (K). The quadratic form of Eq. (1) was chosen over a linear fit because of better accuracy, especially at extreme values. The intercept of the nonlinear fit is forced to be zero, since physically $T_f = 0$ when $T_w = 0$. In the operational processing of the NOAA observations, the nadir window radiance is obtained from the observed radiance by means of a limb darkening correction, which is also based on a regression equation derived from radiative transfer calculations (Abel and Gruber, 1979).

For our observational data sets, we fitted the quadratic, zero intercept form of Eq. (1) to the data, as well as linear and full quadratics. We obtain T_w from the THIR window radiance observations from the calibration of the THIR instrument (NASA, 1982), and T_f from the ERB radiance observations by first converting these (approximately) nadir radiances to fluxes by application of a limb darkening function, and then inverting the Stefan–Boltzmann equation to retrieve the flux equivalent temperature T_f. The coefficients for the limb darkening function used are given in the supplement (Wark *et al.*, 1963) to Wark *et al.* (1962); they are derived from radiative transfer calculations of the type discussed above. Using this limb darkening function, the flux F can be obtained from the nadir radiance, $R(0)$, through the equation

$$F = R(0)[3.247 - 2.457 \times 10^{-3}R(0)], \qquad (2)$$

where $R(0)$ is in units of W m^{-2} sr^{-1} and F is in W m^{-2}. Several fits were also made without application of the limb darkening function. In this case, the radiance is assumed to be isotropic, which leads to $F = \pi R(0)$.

3. Results

Figure 1 shows plots of the quadratic equations obtained by applying least-squares regression analysis to each of the three observational data sets. Also shown

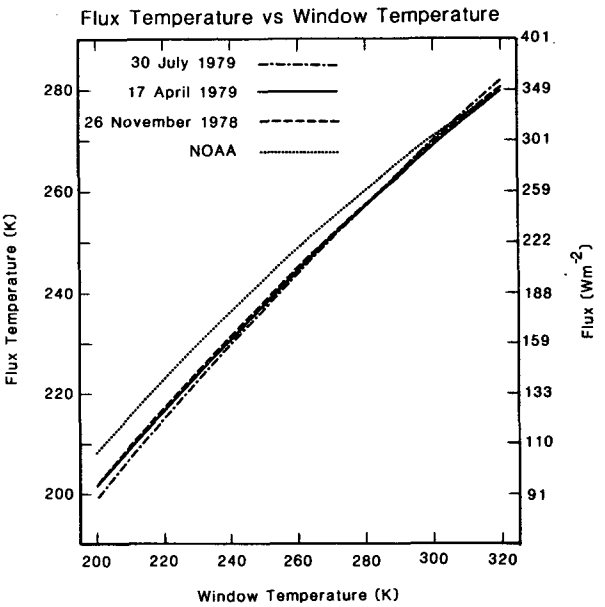

FIG. 1. Empirical (17 April 1979, 30 July 1979, and 26 November 1978) and theoretical (NOAA) regression equations relating flux equivalent brightness temperature T_f to window radiance equivalent brightness temperature T_w.

is the theoretical quadratic equation that was used operationally for one of the NOAA satellites. There are some minor differences in the operational equation from satellite to satellite because of small differences in the instrument filters. The ordinate in this graph is the flux equivalent brightness temperature, and the abscissa is the window radiance equivalent brightness temperature. The coefficients for these regression equations, as well as those for all the other regression equations discussed in this paper, are summarized in Table 1. The curves from the observational data are quite consistent with one another, two of them, for 26 November 1978 and 17 April 1979, being almost identical. These empirically derived curves differ systematically from the NOAA operational curve, the NOAA flux temperatures being higher except for very high fluxes. This difference is consistent with the observed positive bias of the NOAA longwave fluxes compared to broad-band observations (see, for example, Ohring and Gruber, 1983). Each of the observational curves has a standard error of estimate of ~3°C. The linear fits had a slightly larger error, while the full quadratic had about the same error.

As indicated earlier, the ERB radiances were converted to fluxes by means of a limb darkening function. Figure 2 shows the effect of the limb darkening on the relationship between the flux temperature and the window temperature. The isotropic curve is derived assuming no limb darkening. At the higher window temperatures, the flux temperatures are lower for the limb darkened curve than for the isotropic curve. The difference between the two curves decreases with decreasing window temperature and, in fact, at very low window temperatures the flux temperatures for the limb darkened curve are slightly higher than for the isotropic curve—an indication of limb brightening. This behavior derives from the difference between Eq. (2) and the equation for the isotropic case of no limb darkening. Physically, this behavior can probably be explained as follows. At high window temperatures, such as occur in the tropics, limb darkening is greatest due to generally increased water vapor amounts and greater lapse rates. At low window temperatures, such as occur in polar regions or in the case of very high, thick clouds, water vapor amounts are small. In these cases, limb brightening could result from deep surface inversions in polar regions and from stratospheric carbon dioxide and ozone emission above very high, thick clouds in the tropics. In any case, the curves shown in Fig. 2 suggest that the difference between the empirical and NOAA operational curves of Fig. 1 do not depend on the exact form of the limb darkening function.

TABLE 1. Values of coefficients a and b in regression equations discussed in the present study.

Source	a	b (K^{-1})
17 April 1979	1.228	-1.106×10^{-3}
30 July 1979	1.187	-9.566×10^{-4}
26 November 1978	1.228	-1.098×10^{-3}
NOAA SR (Abel and Gruber, 1979)	1.3185	-1.387×10^{-3}
Ellingson–Ferraro (1982)	1.2736	-1.231×10^{-3}
Three-day data set	1.215	-1.055×10^{-3}
17 April 1979, isotropic	1.197	-9.676×10^{-4}

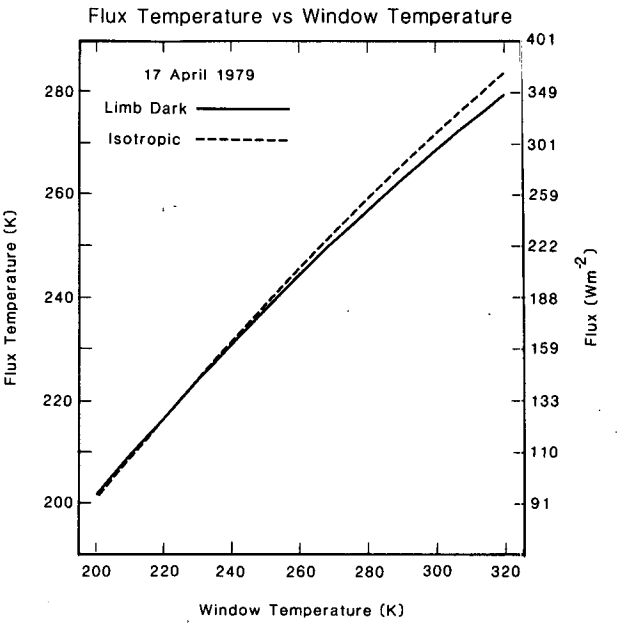

FIG. 2. Empirical regression equations relating T_f to T_w for two cases, 17 April 1979 (see text for explanation): 1) limb darkening; 2) no limb darkening (isotropic).

Recently, Ellingson and Ferraro (1983) have redone the Abel and Gruber (1979) simulations of flux and window radiance from model atmospheres. The new calculations use improved spectral transmission data, provide for partial cloudiness in the field of view, and permit cirrus clouds to have spectrally varying emissivities. Figure 3 compares the NOAA regression equation, the Ellingson–Ferraro (1983) equation, and an equation derived by combining the three days of Nimbus-7 observational data into one data set. While the new relationship reduces the positive bias of the NOAA equation over most of the range of observations, it actually increases it at high flux values.

It is not obvious why the theoretical equations have a positive bias with respect to the empirical equations. The bias in flux equivalent brightness temperature is such that it is close to zero at high values of window radiance equivalent brightness temperature, and increases with decreasing values of window temperature. The relative bias would be close to zero at window temperatures of 310 K, ~1.5% at a window temperature of 270 K, and ~3% at a window temperature

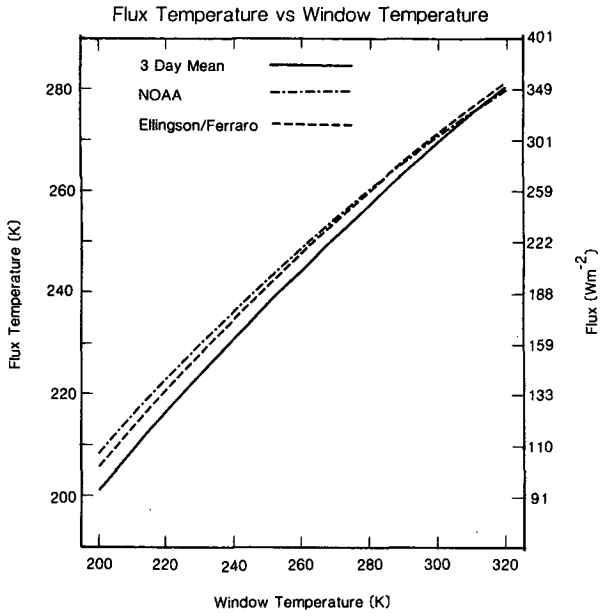

FIG. 3. Empirical (three-day combined sample) and theoretical (NOAA and Ellingson and Ferraro, 1983) regression equations relating T_f to T_w.

of 220 K. Since, from the Stefan–Boltzmann law, $dF/F = 4dT_f/T_f$, the relative biases in total flux would be four times those in flux equivalent brightness temperature.

To obtain some idea of the errors that might result from the application of the empirical equations to independent data, the following experiment was performed. The coefficients derived from each of the three days of Nimbus-7 data were applied to the IR window observations of the other two days, and the errors in flux equivalent brightness temperature were calculated. The results are shown in Table 2. Also shown in Table 2 are: 1) the errors in flux, which are obtained from the errors in T_f by multiplication by dF/dT_f evaluated at the average value of $T_f = 250$ K, which is 3.54; and 2) the errors resulting from application of the NOAA SR and Ellingson–Ferraro coefficients derived from radiative transfer calculations. The errors resulting from the use of the empirical coefficients are quite stable. The mean or systematic error is close to zero—a fraction of a degree in T_f and 1–2 W m^{-2} in flux—and the rms errors are ~11 W m^{-2}. The NOAA SR coefficients lead to a positive bias of 3.5–3.8 K in T_f, or 12–13 W m^{-2} in flux, and rms errors of 17–19 W m^{-2}. The Ellingson–Ferraro coefficients lead to a reduction of ~3 W m^{-2} in the positive bias and rms errors of 15 W m^{-2}. Thus, although the use of the Ellingson–Ferraro coefficients would reduce somewhat the bias of the NOAA radiation observations, a positive bias of ~10 W m^{-2} would still remain.

It is of interest to compare results from the application of the empirical algorithm, the Ellingson–Ferraro (1983) algorithm, and the NOAA operational algorithm. For this purpose, all three algorithms were applied to three consecutive orbits of high resolution NOAA-6 data. The operational model was derived similarly to the scanning-radiometer data using the methods of Abel and Gruber (1979), and resulted in coefficients that were nearly the same as the pre TIROS-N scanning radiometers. This is, of course, not surprising since the spectral intervals of the radiometer were also similar. Only three orbits of data were compared for the following reasons:

(1) These three orbits represent an experimental data set for research and development and were readily available to us.

(2) We felt that three complete orbits contain enough variability to give us representative results of the application of the improved algorithms.

TABLE 2. Errors in flux equivalent brightness temperature (K) and longwave flux (W m^{-2}) from application of regression equations based on observations and simulations.

Coefficients from:	Coefficients applied to:	Errors					
		Mean		Random		rms	
		K	W m^{-2}	K	W m^{-2}	K	W m^{-2}
17 Apr 79	30 Jul 79	0.08	0.28	3.09	10.9	3.09	10.9
26 Nov 78	30 Jul 79	0.67	2.37	3.06	10.8	3.13	11.1
NOAA SR	30 Jul 79	3.83	13.6	3.65	12.9	5.29	18.7
Ellingson–Ferraro	30 Jul 79	3.20	11.3	3.24	11.5	4.55	16.1
30 Jul 79	17 Apr 79	−0.28	−0.99	3.06	10.8	3.07	10.9
26 Nov 78	17 Apr 79	0.46	1.63	2.95	10.4	2.99	10.6
NOAA SR	17 Apr 79	3.78	13.4	3.22	11.4	4.97	17.6
Ellingson–Ferraro	17 Apr 79	3.05	10.8	2.99	10.6	4.27	15.1
17 Apr 79	26 Nov 78	−0.50	−1.77	3.02	10.7	3.06	10.8
30 Jul 79	26 Nov 78	−0.71	2.51	3.09	10.9	3.17	11.2
NOAA SR	26 Nov 78	3.48	12.3	3.25	11.5	4.76	16.8
Ellingson–Ferraro	26 Nov 78	2.70	9.6	3.06	10.8	4.08	14.4

The application of the algorithms was made to both day and night flux values; however, the results were essentially the same, and so examples from daytime only will be reported. Also, the NOAA-6 window temperatures were adjusted to account for the differences in the spectral response of the THIR and NOAA-6 radiometers. The data were processed into 2.5° latitude by 2.5° longitude grids as is done in the normal operational processing (Gruber and Winston, 1978).

To help interpret the differences between the various algorithms it is useful to examine the emitted flux based on the operational model. This is shown in Figs. 4a and b, which show a map view and zonal averages, respectively, for 13 April 1981 of the daytime emitted flux. From Fig. 4a we see that the three orbits occupy about 75° longitude and extend from Europe and Africa on the eastern boundary to South America on the western boundary. Thus, there is a fairly good rep-

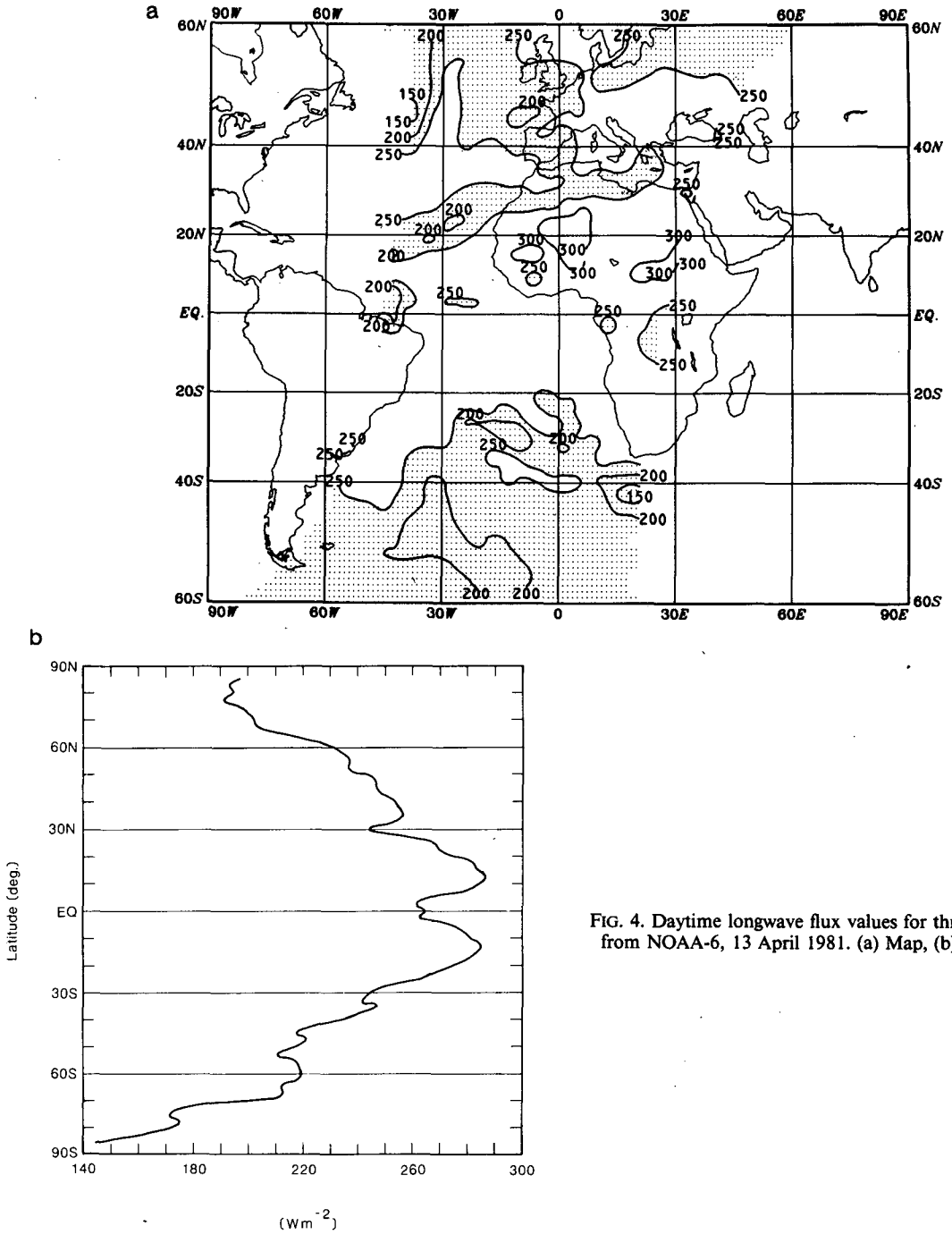

FIG. 4. Daytime longwave flux values for three orbits of data from NOAA-6, 13 April 1981. (a) Map, (b) zonal average.

resentation of land, cloud and ocean. The range of outgoing longwave radiation is from about 150 W m^{-2}, to somewhat in excess of 300 W m^{-2} over Africa. Figure 4b represents zonal averages over the limited longitudinal domain of data, and extending from the North Pole to the South Pole. The largest outgoing flux is found over the relatively cloud-free zones of the subtropical high pressure regions (10–20 N, S), and the minimums are found in the polar regions. Relative minimums at other latitudes are associated with clouds,

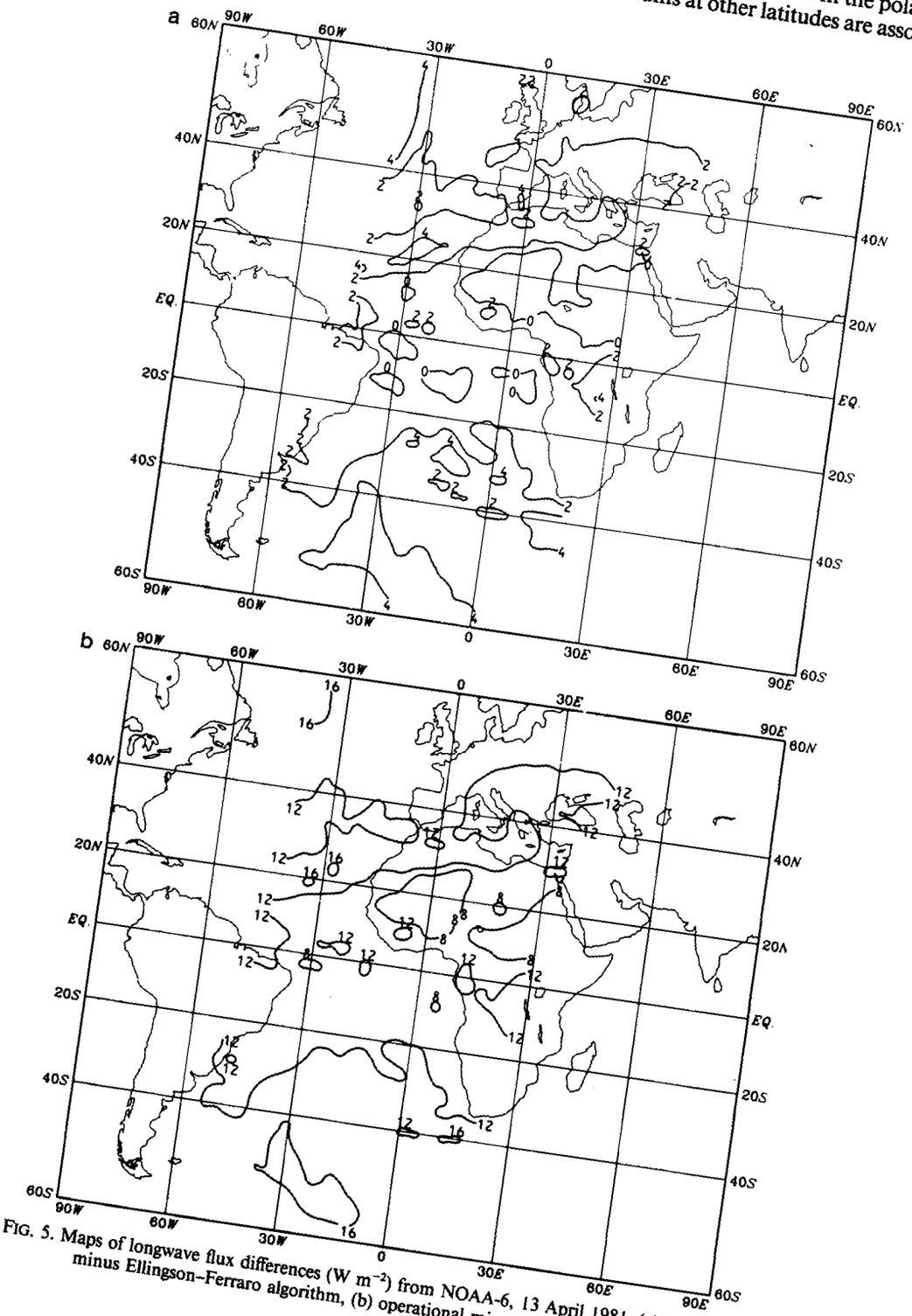

FIG. 5. Maps of longwave flux differences (W m^{-2}) from NOAA-6, 13 April 1981. (a) Operational minus Ellingson–Ferraro algorithm, (b) operational minus empirical algorithm.

the most pronounced minimum occurring near the equator.

Figure 5a is a map of the longwave flux difference: operational minus the Ellingson–Ferraro (EF) algorithm. The largest positive differences are slightly in excess of 4 W m^{-2}, and they occur in low emitting temperature regions, e.g., regions of extensive high cloud or high latitudes. Note particularly the large positive difference (>4 W m^{-2}) located at 20°N, 30°W. This is clearly associated with the high cloudiness inferred from Fig. 4a. Negative differences are found over Africa at about 20°N. This is consistent with the results of Fig. 3 which show a cross-over at flux equivalent temperatures of about 265 K, corresponding to flux values of approximately 280 W m^{-2}. Also, various portions of the equatorial Atlantic exhibit values slightly less than zero.

Figure 5b shows the longwave flux difference between the operational and the empirical algorithm. In terms of spatial distribution it is quite similar to Fig. 5a; however, the differences are much larger. Maximum differences are about 16 W m^{-2} and minimum differences are between 4 and 8 W m^{-2}. Note that there are no negative differences, consistent with Fig. 3 which indicates a crossover at flux equivalent temperatures of about 275 K, corresponding to an emitted flux of about 325 W m^{-2}.

Zonal averages of the differences for the two cases are shown in Fig. 6 and can be compared to the zonal average flux in Fig. 4b. These profiles are consistent with the results shown in Fig. 3, i.e., largest differences over low temperature regions and smallest differences over warm emitting surfaces. The relative maximum near the equator is due to cloudiness associated with the ITCZ. The similarity in the spatial distribution of the differences between the two models, as well as the differences in magnitude, are clearly evident.

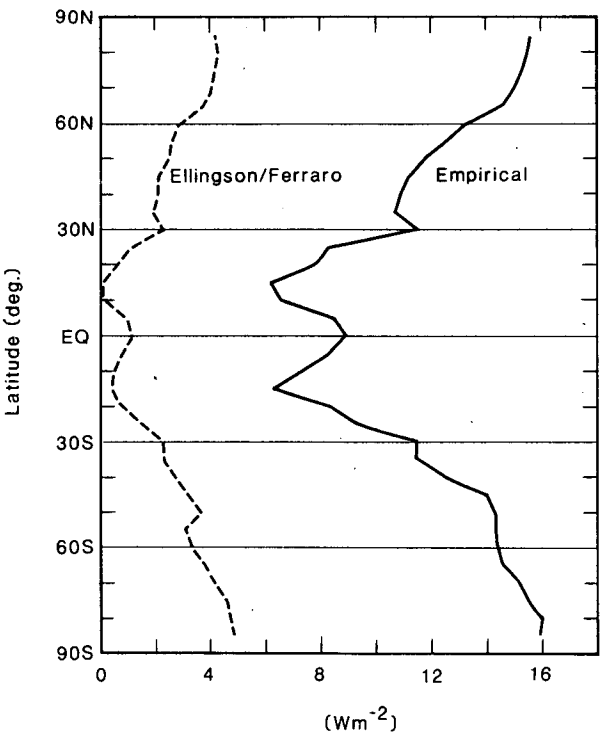

FIG. 6. Zonal-average longwave flux differences, 13 April 1981.

TABLE 3. Means, standard deviations and maximum and minimum differences in longwave flux (W m^{-2}) for three orbits of NOAA-6 data on 13 April 1981: operational minus the Ellingson–Ferraro and empirical models.

	Mean	Standard deviation	Maximum	Minimum
Ellingson–Ferraro	3.1	1.6	5.0	−2.0
Empirical	12.9	3.4	16.3	1.5

An overall summary of the results is given in Table 3 which shows the mean and standard deviation of the differences, and the maximum and minimum differences for the two algorithms, based on all the grid points. When weighting the average differences by area, as would normally be done when computing global averages, the mean differences are about 2.6 W m^{-2} for the Ellingson–Ferraro model, and about 11 W m^{-2} for the empirical model.

In concluding this section it should be pointed out that the empirical model results in two important characteristics. It reduces the average outgoing longwave radiation by almost 11 W m^{-2}, which is approximately the difference between the global average emitted flux based on NOAA operational data and Nimbus-6 ERB data as described by Ohring and Gruber (1983). The present results are of course not for global averages but it is reasonable to assume no significant change when extended over the globe. The other important characteristic is that the largest differences occur in the low emitting temperature regions, and the smallest differences in the high emitting temperature regions, a pattern that generally follows the differences between the operational estimate and Nimbus-6 measurements of the emitted radiation. This implies that the meridional gradient of outgoing longwave radiation is underestimated somewhat by the operational estimates. Routine application of the empirical algorithm should result in closer agreement between the two on both global and zonal averages. We anticipate that closer agreement will also result on smaller scales.

4. Possible explanations for the empirical–theoretical differences

We have attempted to isolate possible reasons for the differences between the theoretical and empirical flux estimation equations by reexamining different aspects of the observations and calculations. First, it

should be noted that the total longwave radiance R used in Eq. (2) has been estimated from observations of the radiance in the 4–50 μm region, R_f, which has been filtered by the responsivity of the instrument. The ERB estimation is accomplished with the use of an equation of the form

$$R = c + dR_f, \tag{3}$$

where the coefficients were determined from a regression analysis of the radiance calculations of Wark *et al.* (1962) applied to the ERB filter function. We have also computed these coefficients for the ERB instrument using the nadir radiance calculations of Ellingson and Ferraro (1983) (denoted EF) with the same data and cloudiness assumptions used by Wark *et al.* (1962) (our regression analysis results in 99.94% explained variance). When the same nadir filtered radiance is used with the different sets of coefficients for Eq. (3), the results show that fluxes based on the EF coefficients exceed the ERB fluxes by approximately 4 W m^{-2}. Overall, approximately 30% of the mean bias between the empirical and theoretical (EF) estimates is due to the differences in the estimates of the total radiance.

Although a portion of the positive bias of the theoretical equations relative to the empirical results may be explained by the estimation of the unfiltered radiance, an explanation for the remaining positive bias, and its increasing magnitude with decreasing window temperature, is not obvious. If one assumes that the radiance observations are correct, then the conditions that would lead to such a positive bias in flux are underestimates of the calculated window radiation relative to the remainder of the spectrum, and overestimates of the total flux. The fact that the relative bias in flux increases with decreasing flux values could be interpreted as follows. The simulations are omitting the effect of an atmospheric absorbing constituent that is negligible relative to that of water vapor for high flux values (which are usually associated with large water vapor amounts), but becomes important at lower flux values (associated with low water vapor amounts). Similarly, if there were overestimates of the transmission by carbon dioxide, these would be magnified as the water vapor content decreased. Although aerosols are not included in the simulations, their omission would, if anything, cause a bias in the opposite direction, since they can be expected to cause a greater reduction in window brightness temperature than in the total flux equivalent temperature.

An alternative explanation for differences between the empirical and theoretical flux estimates is that the set of soundings used in the calculations is an unrepresentative sample of the mean atmosphere. If it is assumed that the three-day empirical relationship is representative of the mean atmosphere, then the difference between the empirical and theoretical flux estimates could be interpreted as indicating that the soundings are too warm relative to the surface, particularly in regions of cold surfaces. This interpretation can easily be checked by doing calculations with another set of atmospheric data (which we are in the process of doing).

Through an examination of the individual soundings, and through comparisons of mean soundings with standard atmospheres, we have determined that the soundings used in the calculations are not representative of the mean atmospheric conditions. In particular, our examination of the individual soundings shows that 70% of the soundings have temperature inversions at the surface or in the lower troposphere, several soundings have very high stratospheric temperatures, and the water vapor content of the stratosphere greatly exceeds that normally assumed. All of these peculiarities lead to increased fluxes relative to the values that would be calculated if the tropospheric temperatures decreased monotonically with altitude.

The average soundings for 0–30, 30–60, and 60–90°N were compared to the McClatchey *et al.* (1972) tropical, and summer and winter midlatitude and subarctic standard atmospheres. The comparisons show that the soundings are colder in the lower troposphere (pressures > 500 mb) than in the standard atmospheres by approximately 3°C in the tropics (16 cases) and up to 12°C in the subarctic summer (12 cases). In addition, the temperature difference between 1000 and 150 mb for the standard atmosphere exceeds that for the soundings by 2.7°C in the tropics, 4.1°C in the midlatitude summer (33 cases), and 19.5°C in the subarctic summer. These differences are in the correct direction to explain the sign of the bias of the EF fluxes relative to the empirical values.

As a test of effects of the differences between the mean soundings and standard atmospheres, we have calculated the clear sky upward flux at 70 km (F_C) for each of the standard atmospheres, and we have used the calculated THIR window brightness temperatures (T_R) for these standard atmospheres to compute fluxes with the empirically determined coefficients (F_E), with the EF coefficients (F_T), and with the empirical coefficients modified for the EF unfiltered–filtered radiance relationship (F_M). The differences between the various fluxes, shown in Table 4, reveal a number of important results. First, the differences between the F_T and F_E values are of the same magnitude and sign as shown in Table 2 (approximately 10 W m^{-2}). However, the differences between F_E and F_C are smaller than the differences between F_T and F_C, and these differences are smaller at low, rather than high, brightness temperatures. In view of the latter result, it is not surprising that the differences between F_M and F_C are the smallest of the three sets. That is, the theoretically calculated fluxes for the standard atmospheres agree with those estimated with the modified empirical coefficients better than those estimated with the coefficients determined from theoretical calculations using the atmospheric soundings.

TABLE 4. Calculated and estimated fluxes (W m^{-2}) for different standard atmospheres. F_C, theoretically calculated; F_E, empirical estimate; F_T, Ellingson–Ferraro estimate; F_M, modified empirical estimate. T_R is the calculated THIR window brightness temperature for each standard atmosphere.

Atmosphere	F_C	T_R (K)	$F_E - F_T$	$F_E - F_C$	$F_T - F_C$	$F_M - F_C$
Tropical	289.9	294.8	−8.6	−3.9	4.7	0.2
Midlatitude summer	281.4	291.2	−9.1	−4.5	4.6	−0.7
Midlatitude winter	230.3	271.5	−10.9	−1.2	9.7	1.8
Subarctic summer	265.4	284.7	−9.8	−4.7	5.1	−1.2
Subarctic winter	198.5	256.8	−11.4	−2.6	8.8	0.2

In view of these results we are optimistic that the differences between the empirical and theoretical model coefficients will decrease as the sample of soundings used in the calculations approaches the average conditions sensed by the satellite. However, these results also show the magnitude of the errors which may result when large deviations from average occur. These errors might be decreased, however, with the use of multichannel observations.

5. Discussion and conclusions

Our results indicate that there is indeed a very high correlation between the observed flux equivalent brightness temperature and the observed radiance equivalent brightness temperature of the IR window, and that the former can, therefore, be estimated from measurements of the latter. This conclusion supports the use of the NOAA satellite SR and AVHRR IR window observations for deriving total longwave flux. However, our results suggest that the NOAA values would have a positive bias of $\sim$11 W m^{-2} when globally averaged. This bias is in agreement with that obtained from comparison of large-scale averages of the NOAA longwave fluxes with broad-band longwave observations. It also matches the excess emission to space indicated by the NOAA observations when the annual global mean values of longwave emission and absorption of solar radiation are compared (Ohring and Gruber, 1983).

If we assume that the observations are correct, then the source of the bias must be sought in the simulations using radiative transfer and atmospheric soundings. Our preliminary search for the cause of the bias suggests that the sample of atmospheric soundings used in the theoretical calculations may be unrepresentative. The sample average soundings for the 0–30, 30–60, and 60–90°N latitude belts appear to be systematically different from the standard atmosphere temperature profiles for these regions. The differences are in the correct direction to explain the sign of the bias of the theoretical algorithms, and sample calculations indicate that the magnitude of the bias can also be explained. Recalculation of the theoretical regression coefficients for a larger sample of atmospheric soundings is required to verify this tentative conclusion. In the meantime, it would be appropriate to use empirically derived coefficients of the type described here for future processing of the NOAA data, as well as for the reprocessing of past data. This would provide a continuous radiation budget data set with little or no systematic error (compared to NFOV broad-band observations). Thus, the data from both sources could be combined for various studies, for example, the diurnal variation of longwave flux to space.

The random errors of the empirical and theoretical coefficients are similar, being $\sim$11 W m^{-2}. This value suggests that the use of a longwave flux observation for a single time may not be appropriate for some applications. However, all studies involving monthly averaging and statistical processing should yield reasonably accurate results.

As can be seen from Fig. 3, the slopes of the theoretical relationships between flux equivalent brightness temperature and window radiance equivalent brightness temperature are less than that of the empirical relationship. At an average value of T_w = 270 K, the NOAA SR slope is about 90% of the empirical slope. The difference is larger at higher window temperatures and smaller at lower window temperatures, where the theoretical and empirical slopes approach each other. Thus, on average the range and variability of NOAA SR longwave fluxes can be expected to be some 10% less than that of broad-band fluxes. This would have some effect on numerical results obtained in sensitivity and other diagnostic studies using NOAA SR longwave data, but probably would not influence the major conclusions of such studies.

Acknowledgments. The authors would like to thank Mr. V. Ray Taylor for preparing the datasets, Drs. Larry Stowe and Herbert Jacobowitz for clarification of the procedures used to process the ERB and THIR observations, and Ms. M. Varnadore for her computational and computer-graphics support.

REFERENCES

Abel, P. G., and A. Gruber, 1979: An improved model for the calculation of longwave flux at 11 μm. NOAA Tech. Memo. NESS 106, Washington, DC, 24 pp. [NTIS PB80-119431].

Cahalan, R. F., D. A. Short and G. R. North, 1982: Cloud fluctuation statistics. *Mon. Wea. Rev.*, **110**, 26–43.

Ellingson, R. G., and R. R. Ferraro, Jr., 1983: An examination of a technique for estimating the longwave radiation budget from

satellite radiance observations. *J. Climate Appl. Meteor.*, **22**, 1416–1423.

Fromm, M. D., L. M. Penn, J. J. Cahir and H. A. Panofsky, 1982: Statistical estimates of monthly mean and interannual changes of radiation fluxes at the top of the atmosphere. *J. Atmos. Sci.*, **39**, 1545–1554.

Gruber, A., 1977: Determination of the Earth–atmosphere radiation budget from NOAA satellite data. NOAA Tech. Rep. NESS 76, Washington, DC, 28 pp. [NTIS PB279-633].

——, and J. S. Winston, 1978: Earth–atmosphere radiative heating based on NOAA scanning radiometer measurements. *Bull. Amer. Meteor. Soc.*, **59**, 1570–1573.

Hartmann, D. L., and D. A. Short, 1980: On the use of earth radiation budget statistics for studies of clouds and climate. *J. Atmos. Sci.*, **37**, 1233–1250.

Heddinghaus, T. R., and A. F. Krueger, 1981: Annual and interannual variations in outgoing longwave radiation over the tropics. *Mon. Wea. Rev.*, **109**, 1208–1218.

Jensenius, J. A., J. J. Cahir and H. A. Panofsky, 1978: Estimation of outgoing longwave radiation from meteorological variables accessible from numerical models. *Quart. J. Roy. Meteor. Soc.*, **104**, 119–130.

Liebmann, B., and D. L. Hartmann, 1982: Interannual variations of outgoing IR associated with tropical circulation changes during 1974–78. *J. Atmos. Sci.*, **39**, 1153–1162.

McClatchey, R. H., R. W. Fenn, J. E. A. Selby, F. E. Volz and J. S. Garing, 1972: Optical properties of the atmosphere. AFCRL-72-0497, Air Force Cambridge Research Laboratories, 108 pp. [NTIS-AD753075].

NASA, 1978: Nimbus-7 users' guide. C. R. Madrid, Ed., NASA/Goddard Space Flight Center, Greenbelt, MD, 263 pp. + Appendices.

——, 1982: Nimbus-7 Temperature Humidity Infrared Radiometer (THIR) data users' guide. P. H. Hwang, Ed., NASA/Goddard Space Flight Center, Greenbelt, MD, 52 pp. + Appendices.

Ohring, G., and P. Clapp, 1980: The effect of changes in cloud amount on the net radiation at the top of the atmosphere. *J. Atmos. Sci.*, **37**, 447–454.

——, and A. Gruber, 1983: Satellite radiation observations and climate theory. *Advances in Geophysics*, Vol. 25, Academic Press, 237–304.

Stowe, L. L., T. S. Chen, H. Jacobowitz and I. Ruff, 1978: Classification of clouds for the Nimbus satellite ERB experiment using THIR data. *Preprints Third Conf. Atmospheric Radiation*, Davis, Amer. Meteor. Soc., 103–106.

Wark, D. Q., G. Yamamoto and J. Lienesch, 1962: Infrared flux and surface temperature determinations from TIROS radiometer measurements. Meteor. Sat. Lab. Rep. 10, U.S. Dept. Commerce, Weather Bureau, Washington, DC, 84 pp.

——, —— and ——, 1963: Infrared flux and surface temperature determinations from TIROS radiometer measurements. Meteor. Sat. Lab. Rept. 10, Suppl., U.S. Dept. Commerce, Weather Bureau, Washington, DC, 6 pp.

Winston, J. S., and A. F. Krueger, 1977: Diagnosis of the satellite observed radiative energy in relation to the summer monsoon. *Pure Appl. Geophys.*, **115**, 1131–1144.